Progress In Electromagnetics Research M, Vol. 110, 61–72, 2022

Compressed T-Matrix Algorithm for Scalar and Electromagnetic Scattering from Multiple Objects and Multiple Incident Directions

Mark S. Haynes* **and Ines Fenni**

Abstract—A compression algorithm for the T-matrix scattering solution from multiple objects and incident fields is derived and examined which we call the Compressed T-Matrix Algorithm (CTMA). The CTMA is derived by applying the SVD and Woodbury matrix-inverse identity to compress the original T-matrix system of equations and simultaneously compress the matrix of right-hand side incident field vectors. This is suited for scattering problems with many incident directions. We quantify the compression rates for different collections of dielectric spheres and draw comparisons to the Characteristic Basis Function Method (CBFM) with which the CTMA shares many structural similarities.

1. INTRODUCTION

The T-matrix formulation is one of many ways to compute the multiple scattering solutions of a collection of objects [1–3]. The solutions usually start by assuming that the T-matrix of each object in isolation is known. The fields in each object frame are related through the wave function translation matrices to build a linear system of equations for the scattered field coefficients of each object. Numerous versions of T-matrix multiple scattering algorithms exist including the standard formulation [4], recursively aggregate T-matrix methods [2, 5, 6] and T-matrix interaction matrices [7, 8]. T-matrix methods are attractive for computing the scattering from a collection of spheres because the T-matrix of a sphere is diagonal [6, 9–11]. One drawback of T-matrix methods is that the computation of the translation matrix addition theorems creates restrictions depending on the form of the algorithms. For example, constraints exist on the radii at which new scatterers are added in recursive aggregation [6] as well as the smallest distance between scatterers [12].

The standard T-matrix multiple scattering solution, as opposed to recursive or aggregate methods, builds and solves a linear system of interaction equations for the scattered field expansion coefficients of each scatterer for every incident field [4, 10]. The linear system can be solved with 1) matrix inversion, 2) using iterative methods, and possibly accelerated with techniques like the Fast Multipole Method [4], or 3) direct solvers such as LU decomposition, which are suitable to multiple right hand sides (RHSs). Multiple right hand sides, i.e., multiple incident fields, numbering in the tens of thousands are often required in the estimation of average scattering quantities, depending on the size of the object [13–15], or in the analysis of 3D radar scattering of large targets.

In this work, we derive and examine a compression scheme for the standard T-matrix scattering solution called the Compressed T-Matrix Algorithm (CTMA). The purpose of the CTMA is to solve larger T-matrix problems while simultaneously accommodating many incident fields. Our approach is a straightforward application of the SVD and Woodbury matrix-inverse identity which are used together to construct a compressed system of equations for the spherical harmonic expansion coefficients of the scattered field for each object. Like most T-matrix algorithms, it assumes that each object has a known

Received 9 March 2022, Accepted 18 April 2022, Scheduled 27 April 2022
* Corresponding author: Mark S. Haynes (Mark.S.Haynes@jpl.nasa.gov).
The authors are with the Jet Propulsion Laboratory, California Institute of Technology, USA.

isolated T-matrix. The CTMA shares many similarities with the Characteristic Basis Function Method (CBFM) [16], or the Adaptive Cross Approximation (ACA) algorithm [17], where these algorithms seek the effective rank of the matrix to take advantage of the difference between the true rank and effective rank to compress the core interaction matrix in a way that is also suitable for multiple RHSs.

In Section 2, we outline the standard T-matrix scattering solution for scalar and vector waves. In Section 3, we derive the CTMA. Section 4 contains examples of the algorithm and performance comparisons against the standard solution. Finally, Section 5 contains discussion about the relationship between this algorithm and the MoM and CBFM solutions as well as a variant useful for parametric studies in static geometries.

2. STANDARD T-MATRIX SCATTERING SOLUTION

In this section, we give the equations for the standard scalar and vector T-matrix multiple scattering problems. The geometry is shown in Figure 1.

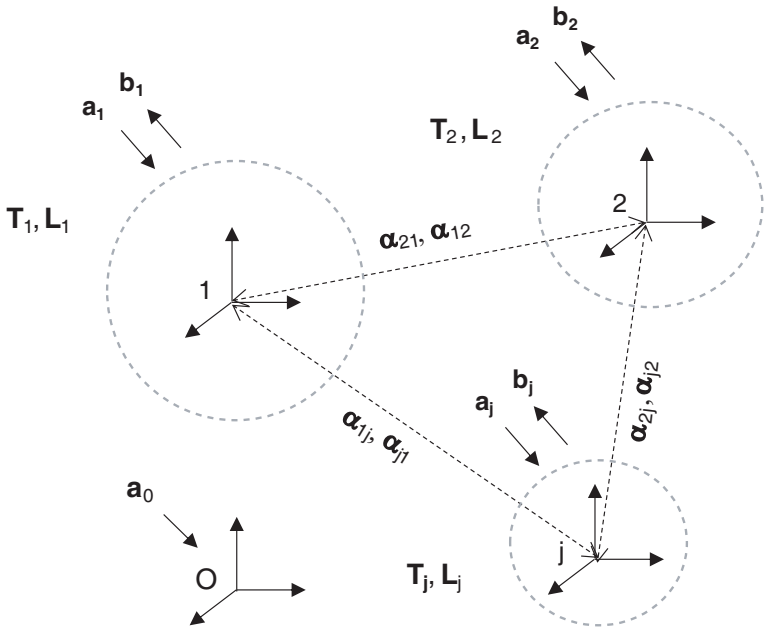

Figure 1. Geometry of T-matrix multiple scattering solution. Each object frame is at location $\mathbf{r}_i$ in the global frame. The isolated object T-matrix, $\mathbf{T}_i$, is given with harmonic content up to maximum degree $L \sim O(ka)$ which can be different for each object. Translation matrices, $\boldsymbol{\alpha}_{ji}$, link the field expansions between object frames. The incident and scattered expansion coefficients in each frame are $\mathbf{a}_j$ and $\mathbf{b}_j$, respectively.

2.1. Scalar Waves

A linear system of equations for the scattering of multiple objects using the T-matrix is derived for scalar waves in [2, 4]. We repeat the main points of the derivation here. Let n objects be centered at locations $\mathbf{r}_i$ in a background medium with wavenumber k. The total field around the collection of objects is written as

$$\phi_{tot}(\mathbf{r}) = \phi_{inc}(\mathbf{r}) + \phi_{sca}(\mathbf{r}) \tag{1}$$

$$= Rg\boldsymbol{\psi}^t(k, \mathbf{r}) \cdot \mathbf{a}_0 + \sum_{i=1}^{N} \boldsymbol{\psi}^t(k, \mathbf{r}_i) \cdot \mathbf{b}_i \tag{2}$$

where $\mathbf{r}$ is the position vector in the global frame centered at the origin; $\mathbf{r}_i$ is the position vector relative to the frame of object i; $\mathbf{a}_0$ are the incident field expansion coefficients in the global frame; $\mathbf{b}_i$ are the

scattered field coefficients of object i; and $Rg\boldsymbol{\psi}(k,\mathbf{r})$ and $\boldsymbol{\psi}(k,\mathbf{r})$ are the regular and radiating scalar wave functions written in vector notation and given by [2]

$$Rg\psi_{lm}(k,\mathbf{r}) = j_l(kr)Y_{lm}(\theta,\phi) \tag{3}$$

$$\psi_{lm}(k,\mathbf{r}) = h_l^{(1)}(kr)Y_{lm}(\theta,\phi) \tag{4}$$

where $j_l(kr)$ and $h_l^{(1)}(kr)$ are spherical Bessel and Hankel functions, respectively; $Y_{lm}(\theta,\phi)$ are the spherical harmonics; k is the background wavenumber; and Rg means being regular (non-singular) at the origin.

Using the translation matrices for the scalar spherical wave functions [18–20], the incident field is first translated to the frame of the jth scatterer, and second, the scattered fields from $n-1$ scatterers are translated as incoming fields in the frame of the jth scatterer as

$$\phi_{tot}(\mathbf{r}_j) = Rg\boldsymbol{\psi}^t(k,\mathbf{r}_j)\cdot\boldsymbol{\beta}_{j0}\cdot\mathbf{a}_0 + \sum_{i=1,i\neq j}^{n} Rg\boldsymbol{\psi}^t(k,\mathbf{r}_i)\cdot\boldsymbol{\alpha}_{ji}\cdot\mathbf{b}_i + \boldsymbol{\psi}^t(k,\mathbf{r}_j)\cdot\mathbf{b}_j \tag{5}$$

where $\boldsymbol{\alpha}_{ji}$ is the translation matrix pointing from frame i to frame j that contains radiating Hankel functions, and $\boldsymbol{\beta}_{j0}$ is the translation matrix between global origin and frame j that contains Bessel functions. The first two terms of Eq. (5) act like a combined incident field on the jth scatterer. We relate $\mathbf{b}_j$ to the incident field coefficients in the frame of the scatterer, $\mathbf{a}_j = \boldsymbol{\beta}_{j0}\cdot\mathbf{a}_0$, through the isolated T-matrix of object j, $\mathbf{T}_j$, as

$$\mathbf{b}_j = \mathbf{T}_j\cdot\left(\mathbf{a}_j + \sum_{i=1,i\neq j}^{n}\boldsymbol{\alpha}_{ji}\cdot\mathbf{b}_i\right) \tag{6}$$

Evaluating for $j = 1\ldots n$ we get a linear system of equations for all $\mathbf{b}_j$ in terms of $\mathbf{a}_j$.

$$(\mathbf{I} - \mathbf{T}\cdot\boldsymbol{\alpha})\cdot\mathbf{b} = \mathbf{T}\cdot\mathbf{a} \tag{7}$$

where $\mathbf{I}$ is the identity matrix; $\mathbf{T}$ is a block diagonal T-matrix; $\boldsymbol{\alpha}$ is the full block translation matrix; and $\mathbf{a}$ and $\mathbf{b}$ are the incident and scattered vectors with field coefficients for all scatterers:

$$\mathbf{T} = \begin{bmatrix} \mathbf{T}_1 & & & \\ & \mathbf{T}_2 & & \\ & & \ddots & \\ & & & \mathbf{T}_n \end{bmatrix} \tag{8}$$

$$\boldsymbol{\alpha} = \begin{bmatrix} 0 & \boldsymbol{\alpha}_{12} & \boldsymbol{\alpha}_{13} & & \boldsymbol{\alpha}_{1n} \\ \boldsymbol{\alpha}_{21} & 0 & \boldsymbol{\alpha}_{23} & \ldots & \boldsymbol{\alpha}_{2n} \\ \boldsymbol{\alpha}_{31} & \boldsymbol{\alpha}_{32} & 0 & & \boldsymbol{\alpha}_{3n} \\ & \vdots & & \ddots & \vdots \\ \boldsymbol{\alpha}_{n1} & \boldsymbol{\alpha}_{n2} & \boldsymbol{\alpha}_{n3} & \ldots & 0 \end{bmatrix} \tag{9}$$

$$\mathbf{b} = \begin{bmatrix} \mathbf{b}_1 \\ \mathbf{b}_2 \\ \vdots \\ \mathbf{b}_n \end{bmatrix}, \qquad \mathbf{a} = \begin{bmatrix} \mathbf{a}_1 \\ \mathbf{a}_2 \\ \vdots \\ \mathbf{a}_n \end{bmatrix} \tag{10}$$

Equation (7) can be solved for $\mathbf{b}$ using any linear algebra technique. Once $\mathbf{b}$ is known, the scattered field outside the regions of individual objects is computed with Eq. (2).

Let there be p incident fields from different sources such that (7) is extended to have multiple RHSs, which we write as

$$(\mathbf{I} - \mathbf{T}\cdot\boldsymbol{\alpha})\cdot\mathbf{B} = \mathbf{T}\cdot\mathbf{A} \tag{11}$$

where $\mathbf{A} = [\mathbf{a}^1, \mathbf{a}^2, \ldots, \mathbf{a}^p]$ is the incident field matrix that contains p vectors of incident field coefficients, and $\mathbf{B} = [\mathbf{b}^1, \mathbf{b}^2, \ldots, \mathbf{b}^p]$ is the solution matrix that contains p vectors of scattered field coefficients.

The following observations are relevant for computation:

(i) The sums in the field expansions are technically infinite but are truncated in practice.

(ii) The magnitude of T-matrix elements of any finite object fall off exponentially for harmonics $l > L \sim O(ka)$, where a is the radius of the bounding sphere of the object. The fall off acts like a filter on the translation matrices which allows safe truncation of the sums.

(iii) The maximum degree harmonic required to expand the scattered field of each object is [21]

$$L \geq \lceil 1.2ka \rceil \tag{12}$$

where the total number of harmonics for all l up to L all $\pm m$ is $N = L^2 + 2L + 1$, which includes the monopole term for scalar waves.

(iv) The isolated T-matrices are square, but the number of harmonics for each object can be different; therefore, in general the translation matrices, $\boldsymbol{\alpha}_{ji}$, are rectangular.

(v) The block translation matrix, $\boldsymbol{\alpha}$, is square but not symmetric because the transpose of the translation matrices is asymmetric for certain harmonics. The transpose relations for scalar (and vector) translation matrices are

$$\alpha^{ij}_{l',-m',l,-m} = (-1)^{m-m'} \alpha^{ji}_{lm,l'm'} \tag{13}$$

where ji translates from frame j to i, while ij is the reverse. Equation (13) is used to accelerate building the full translation matrix.

(vi) The global incident field expansion coefficients $\mathbf{a}_0$ need as many harmonics as are required to expand the incident field over the entire domain of scatterers. The translation $\mathbf{a}_j = \boldsymbol{\beta}_{j0} \cdot \mathbf{a}_0$ reduces the number of incident coefficients for each object frame to only those required to expand the incident field around the isolated object. This is the same number of harmonics used for the T-matrices and translation matrices. Alternatively, the expansion coefficients in the frame of each object $\mathbf{a}_j$ can be computed directly from a source rather than translated through the global origin.

(vii) The smallest unit scatterer is a monopole; therefore, the smallest translation matrix is a single element that translates the field between two monopoles.

2.2. Vector Waves

A linear system of equations for the T-matrix scattering solution for vector waves can be derived in a similar manner as for scalar waves by expanding the electric fields of each dielectric object in vector spherical wave functions and then repeat the steps in the previous section. A radiating electric field is expanded

$$\mathbf{E}(\mathbf{r}) = \sum_{l=1}^{\infty} \sum_{m=-l}^{l} a_{lm} \mathbf{M}_{lm}(k, \mathbf{r}) + b_{lm} \mathbf{N}_{lm}(k, \mathbf{r}) \tag{14}$$

where $\mathbf{M}_{lm}(k, \mathbf{r})$ and $\mathbf{N}_{lm}(k, \mathbf{r})$ are the vector spherical wave functions [2]. The resulting system of equations is the same as the scalar case (7), after the following substitutions:

$$\mathbf{I} \to \begin{bmatrix} \mathbf{I} & 0 \\ 0 & \mathbf{I} \end{bmatrix}, \quad \mathbf{T}_i \to \begin{bmatrix} \mathbf{T}_i^{MM} & \mathbf{T}_i^{MN} \\ \mathbf{T}_i^{NM} & \mathbf{T}_i^{NN} \end{bmatrix}, \quad \boldsymbol{\alpha}_{ji} \to \begin{bmatrix} \mathbf{A}_{ji} & \mathbf{B}_{ji} \\ \mathbf{B}_{ji} & \mathbf{A}_{ji} \end{bmatrix}, \quad \mathbf{b}_i \to \begin{bmatrix} \mathbf{c}_i \\ \mathbf{d}_i \end{bmatrix}, \quad \mathbf{a}_i \to \begin{bmatrix} \mathbf{a}_i \\ \mathbf{b}_i \end{bmatrix}$$

where $\mathbf{T}_i^{xy}$ (x and y are M or N) is the block vector T-matrix for the ith scatterer; $\mathbf{A}_{ji}$ and $\mathbf{B}_{ji}$ are the vector translation matrices between scatterers i and j; and $\mathbf{a}_i$ and $\mathbf{b}_i$ and $\mathbf{c}_i$ and $\mathbf{d}_i$ are the coefficients for the incident and scattered fields, respectively, in the frame of the ith scatterer. Additional notes:

(i) The smallest unit scatterer for vector problems is a dipole which requires 3 harmonics $(l, m) = (1, -1), (1, 0), (1, 1)$. The smallest T-matrix and translation matrix between two dipoles therefore consists of four 3×3 block matrices (i.e., a 6×6 matrix).

(ii) We assume that fully normalized vector spherical wave functions and their associated translation matrices are used. The total number of harmonics for all l up to L all $\pm m$ is $N = L^2 + 2L$.

(iii) The 2×2 nature of the block T-matrix, translation matrices and coefficients capture the coupling between $\mathbf{M}_{lm}$ and $\mathbf{N}_{lm}$ vector spherical wave functions. There are twice as many unknowns as the scalar case, and the overall system of equations is four times as large and requires bookkeeping $\mathbf{M}_{lm}$ and $\mathbf{N}_{lm}$ harmonics separately.

3. COMPRESSED T-MATRIX ALGORITHM — CTMA

Here we motivate and derive the CTMA. The full block translation matrix, $\boldsymbol{\alpha}$, can be very large when the number of scatterers is large, or when the scatterers are large and require many harmonics in the translation matrices. In addition, scattering problems with many incident fields require solving Eq. (7) for many RHSs. The approach of the CTMA is to approximate $\boldsymbol{\alpha}$ with a truncated SVD and combine it with the Woodbury identity to compress the T-matrix system of equations with multiple RHSs.[†]

Let the $n \times n$ matrix $\mathbf{T}\boldsymbol{\alpha}$ in Eq. (7) be approximated by a rank-k SVD as

$$\mathbf{T}\boldsymbol{\alpha} \approx \mathbf{U}_k \boldsymbol{\Sigma}_k \mathbf{V}_k^* \tag{15}$$

where $\mathbf{U}_k$ is sized $n \times k$; $\boldsymbol{\Sigma}_k$ is $k \times k$ diagonal; and $\mathbf{V}_k$ is $n \times k$. The number k is chosen by a threshold to keep the dominant singular values (e.g., if the threshold is 1E-3 then $\sigma_k/\sigma_1 \geq 1E-3$). Recall the Woodbury identity [22, 23], for the inverse of a perturbed matrix when the perturbation is decomposed as the product of three matrices

$$(\mathbf{C} + \mathbf{UDV})^{-1} = \mathbf{C}^{-1} - \mathbf{C}^{-1}\mathbf{U}\left(\mathbf{D}^{-1} + \mathbf{VC}^{-1}\mathbf{U}\right)^{-1}\mathbf{VC}^{-1} \tag{16}$$

Comparing this to Eq. (11) and in light of Eq. (15), we identify $\mathbf{C} = \mathbf{I}$, $\mathbf{U} = -\mathbf{U}_k$, $\mathbf{D} = \boldsymbol{\Sigma}_k$, $\mathbf{V} = \mathbf{V}_k^*$, so that the matrix inverse that is needed to solve Eq. (11) is approximated as

$$(\mathbf{I} - \mathbf{T}\boldsymbol{\alpha})^{-1} \approx \mathbf{I} + \mathbf{U}_k\left(\boldsymbol{\Sigma}_k^{-1} - \mathbf{V}_k^*\mathbf{U}_k\right)^{-1}\mathbf{V}_k^* \tag{17}$$

The solution for $\mathbf{B}$ in Eq. (11) is then

$$\mathbf{B} \approx \left(\mathbf{I} + \mathbf{U}_k\left(\boldsymbol{\Sigma}_k^{-1} - \mathbf{V}_k^*\mathbf{U}_k\right)^{-1}\mathbf{V}_k^*\right)\mathbf{TA} \tag{18}$$

The combination of the SVD and Woodbury identity has compressed the original system of equations so that the matrix to be inverted, $\boldsymbol{\Sigma}_k^{-1} - \mathbf{V}_k^*\mathbf{U}_k$, is sized $k \times k$. The application of $\mathbf{V}_k^*$ to $\mathbf{TA}$ compresses the RHSs along rows which is the dimension containing the spherical harmonics. Let $\mathbf{Y} = \mathbf{V}_k^*\mathbf{TA}$ be the $k \times p$ compressed incident field matrix and let $\mathbf{M} = \boldsymbol{\Sigma}_k^{-1} - \mathbf{V}_k^*\mathbf{U}_k$ be the $k \times k$ compressed matrix so that the compressed unknowns are given by $\mathbf{Z} = \mathbf{M}^{-1}\mathbf{Y}$. We first solve the compressed system

$$\mathbf{MZ} = \mathbf{Y} \tag{19}$$

for the unknowns $\mathbf{Z}$ using any method suitable for multiple RHSs (e.g., LU decomposition). Afterwards, $\mathbf{Z}$ is projected back into spherical harmonics as $\mathbf{U}_k\mathbf{Z}$. The solution is completed by summing the two terms of Eq. (18) as

$$\mathbf{B} \approx \mathbf{TA} + \mathbf{U}_k\mathbf{Z} \tag{20}$$

The physical interpretation of Eq. (20) is that the identity matrix in Eq. (18) yields the first-order scattering solution which is the product of the isolated T-matrices with the incident field coefficients. The second term of Eq. (20), which requires the matrix inverse in Eq. (17), is a correction to the first order solution. This interpretation is consistent with the use of the Woodbury identity as a means to compute a perturbation on a known matrix inverse. In this case, the known inverse is the first order scattering solution where we seek an update that will approximate the full scattering solution. The accuracy of the update is controlled by the truncation threshold of the SVD.

4. EXAMPLES

We test the CTMA, Eq. (20), for the vector electromagnetic problem on a collection of dielectric spheres. We also evaluate compression ratios for different spatial configurations of spheres. The T-matrix for a dielectric sphere is diagonal and given in [24]. The sphere T-matrix and translation matrices for fully normalized vector spherical waves functions are computed using routines in [25].

[†] We drop the dot $(\cdot)$ notation for matrix multiplication in this section.

4.1. Collection Of Spheres

Figure 2 shows a collection of 419 dielectric spheres. The centers of the spheres are distributed uniformly random in XYZ with a 25% fill fraction. The spheres are bounded in a region that is also a sphere that has a diameter of 5λ. The radii of the objects are bounded between 0.1λ and 0.7λ and are approximately distributed according to an exponential distribution. The complex dielectric constant for each sphere is $\epsilon_r = 4 + i0.04$. The number of harmonics used to expand the field of each sphere is determined by the equality condition in Eq. (12). The size of the full translation matrix, $\boldsymbol{\alpha}$, for this problem is 7362×7362.

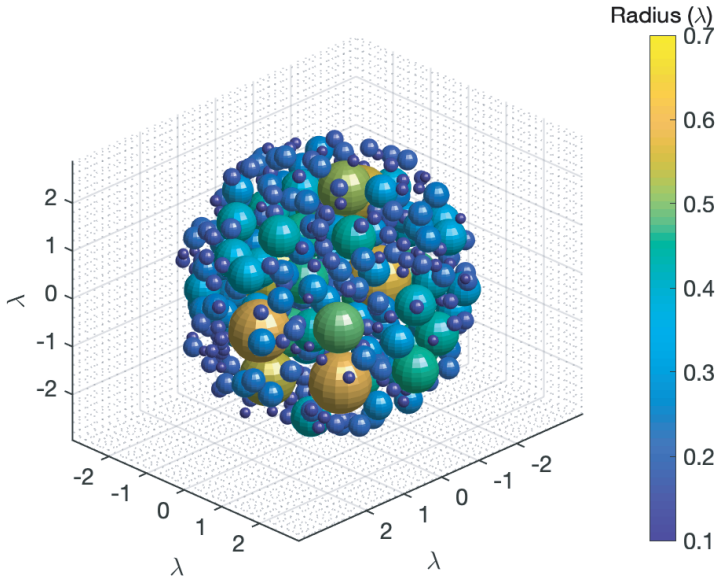

Figure 2. Collection of dielectric spheres to test the compressed T-matrix algorithm against the standard solution. The color maps to sphere radius.

We compute the backscatter radar cross section (BRCS) for 501 incident plane waves at angles arranged uniformly around a circle in the XY plane. The expansion coefficients for plane waves referenced to the origin are given in [25]. These are translated to the frames of each object in order to create the incident field matrix. After the solution is complete, the scattered field expansion coefficients of each object are translated to the origin, summed, and the far-field scattered electric field, which is needed for the BRCS, is computed with the vector spherical harmonics, see also [25]. Figure 3

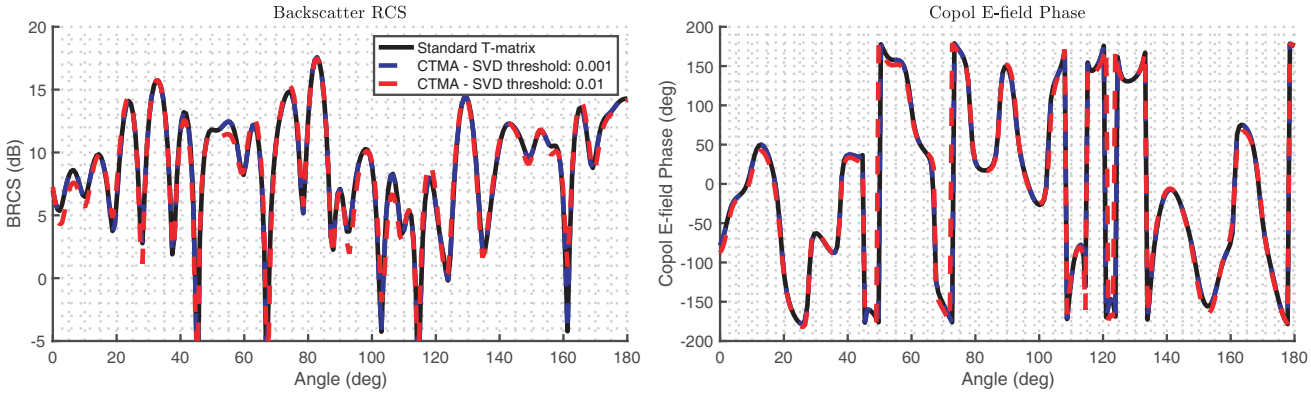

Figure 3. Backscatter radar cross section and co-polarized electric field phase predicted by the standard T-matrix solution and the compressed T-matrix algorithm for different SVD thresholds.

shows the BRCS and the phase of the co-polarized electric field for different SVD thresholds for both the standard solution and CTMA. Most backscatter values are less than about 17 dB. For comparison the BRCS of a solid sphere with $\epsilon_r = 4$ is about 22 dB. We quantify the error between the standard solution and compressed solutions by measuring the RMS of the difference (RMSE) between dB values of backscatter radar cross section over all measurements as well as the RMSE between the phase values of the backscattered electric field. The break point between compression and accuracy is an SVD threshold of about 0.01 which in this example provides an average power error better than 1 dB and average phase error of about 6 degrees with a compression ratio of 35% (see next paragraph) and a speed up in solving the compressed system of about a factor of 3.

The solution of the standard T-matrix system, Eq. (11), for all incident fields took approximately 7.6 seconds to compute in Matlab (2019a) using the backslash operator (condition number 7.3E-5). The one-time SVD, Eq. (15), took approximately 330 seconds to compute. The computation was done on a MacBook Pro OS 11.6 with a 2.9 GHz i9 processor and 32 GB RAM. The compression ratios and times to solve the standard and compressed systems for different SVD thresholds are given in Table 1. The compression ratio measures the relative size of the pre- and post-compressed matrices, namely, $\mathbf{I} - \mathbf{T}\boldsymbol{\alpha}$ and $\boldsymbol{\Sigma}_k^{-1} - \mathbf{V}_k^* \mathbf{U}_k$, respectively. The compression ratio is equal to k^2/n^2 where k is the number of singular values in the compressed system (therefore the number of compressed unknowns), and n is the number of unknowns in the original problem.

Table 1. Performance of the compressed T-matrix Algorithm for different compression ratios.

Singular Value Threshold (σ_k/σ_1)	Compression Ratio (linear)	Computation Time (sec)	BRCS RMSE Power (dB)	E-field RMSE phase (deg)
Standard T-matrix	1	7.6	0	0
0.001	0.78	6.3	0.041	0.27
0.002	0.67	5.3	0.13	0.81
0.005	0.48	3.5	0.4	2.9
0.01	0.35	2.8	0.71	6.2
0.02	0.23	1.8	1.6	11
0.05	0.11	0.91	3.7	36
0.1	0.046	0.42	6.5	60

4.2. Compression Rate For Different Geometries

Here we look at the compression ratios of different geometries of collections of spheres. The compression rate is an indication of the amount of redundancy in the full translation matrix, $\boldsymbol{\alpha}$. Figure 4 illustrates different scenes and geometries, the compression ratios for three SVD thresholds $\sigma_k/\sigma_1 =$ [1E-3, 1E-2, 1E-1], and a plot of normalized singular values. Comparing Case 2 to Case 1 the proposed algorithm compresses better for a similar electrical size but numerically larger problem. Comparing Cases 3 and 4 the compression appears independent of the distance between scatterers for the same size scatterers. Comparing Cases 4 and 5 which are the same sparse geometry with smaller/larger spheres, larger objects, which have more harmonics, compress better. Interestingly the fall off of the singular values for these geometries have similar shapes. This could be due to the square bounding region or the use of the identically sized spheres.

5. DISCUSSION

5.1. Application to The Method Of Moments (MoM)

The combination of SVD and Woodbury identity can be used to compress any linear systems of the form $(\mathbf{I}-\mathbf{A})^{-1}$, as for example in MoM scattering problems where $\mathbf{A}$ is the Green's function interaction matrix. The key difference between the MoM and T-matrix problems is the first order solution. For example, the linear system in the MoM solution of the discretized volume integral equation (VIE) for the total electric field is [25, 26]

$$\left(\mathbf{I}-\begin{bmatrix}\mathbf{G}_{xx} & \mathbf{G}_{xy} & \mathbf{G}_{xz}\\ \mathbf{G}_{yx} & \mathbf{G}_{yy} & \mathbf{G}_{yz}\\ \mathbf{G}_{zx} & \mathbf{G}_{zy} & \mathbf{G}_{zz}\end{bmatrix}\begin{bmatrix}\mathbf{O} & & \\ & \mathbf{O} & \\ & & \mathbf{O}\end{bmatrix}\right)\begin{bmatrix}\mathbf{E}_x\\ \mathbf{E}_y\\ \mathbf{E}_z\end{bmatrix}=\begin{bmatrix}\mathbf{E}_{inc,x}\\ \mathbf{E}_{inc,y}\\ \mathbf{E}_{inc,z}\end{bmatrix} \tag{21}$$

where $\mathbf{I}$ is the identity matrix; $\mathbf{G}_{uv}$ is the Green's function matrix block for pairs of field components; $\mathbf{E}_{inc,v}$ and $\mathbf{E}_v$ are vectors of the incident field and total field solution, respectively; and $\mathbf{O}$ is the diagonal matrix of the object function which is applied to each component. If we apply the compression scheme

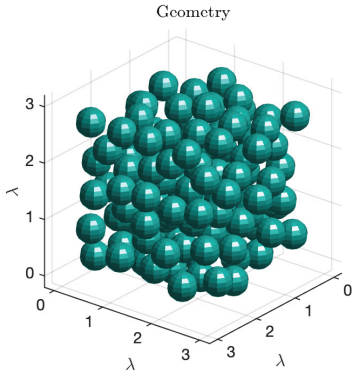

Case	1
N spheres	124
Sphere radii (1)	0.25
Max degree L	2
Nunknowns	1984
Comp. ratio, 1E-3	0.97
Comp. ratio, 1E-2	0.65
Comp. ratio, 1E-1	0.3

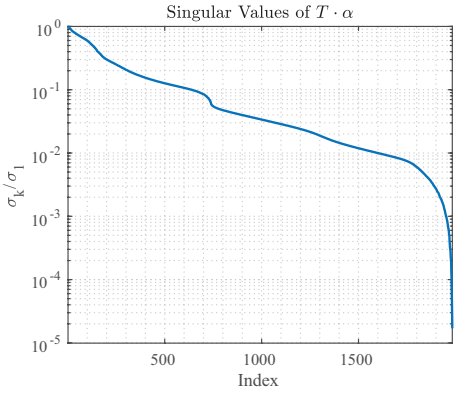

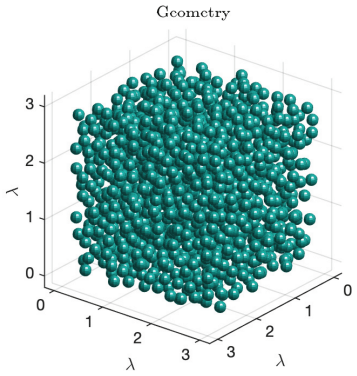

Case	2
N spheres	1290
Sphere radii (λ)	0.1
Max degree L	1
Nunknowns	7740
Comp. ratio, 1E-3	0.97
Comp. ratio, 1E-2	0.25
Comp. ratio, 1E-1	0.01

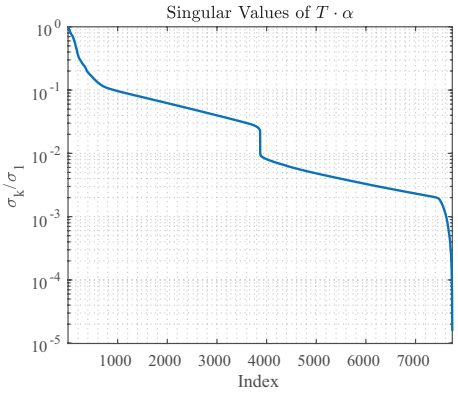

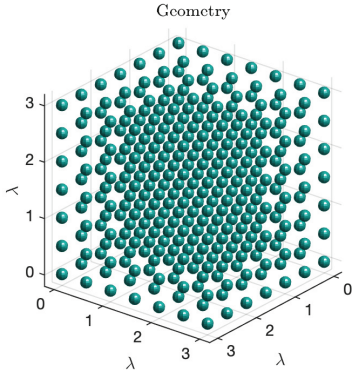

Case	3
N spheres	343
Sphere radii (λ)	0.1
Max degree L	1
Nunknowns	2058
Comp. ratio, 1E-3	0.97
Comp. ratio, 1E-2	0.72
Comp. ratio, 1E-1	0.23

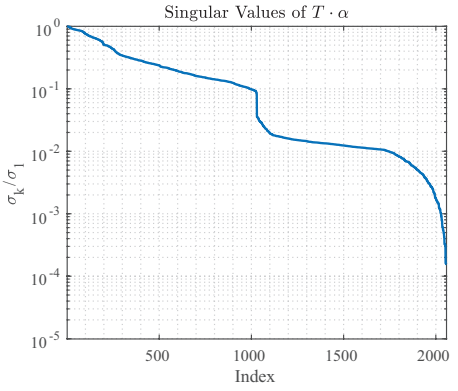

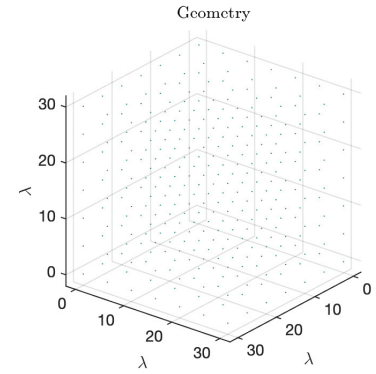

Case	4
N spheres	343
Sphere radii (λ)	0.1
Max degree L	1
Nunknowns	2058
Comp. ratio, 1E-3	0.96
Comp. ratio, 1E-2	0.61
Comp. ratio, 1E-1	0.24

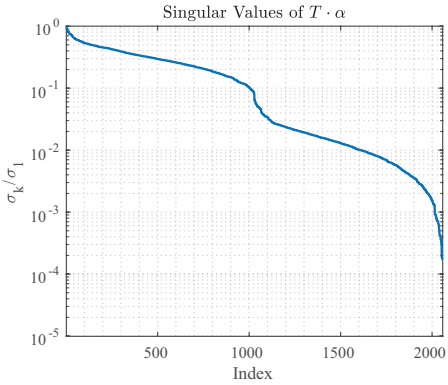

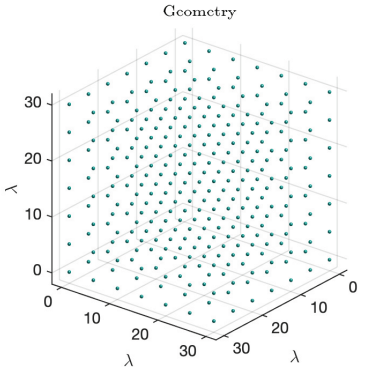

Case	5
N spheres	343
Sphere radii (λ)	0.3
Max degree L	3
Nunknowns	10290
Comp. ratio, 1E-3	0.67
Comp. ratio, 1E-2	0.33
Comp. ratio, 1E-1	0.13

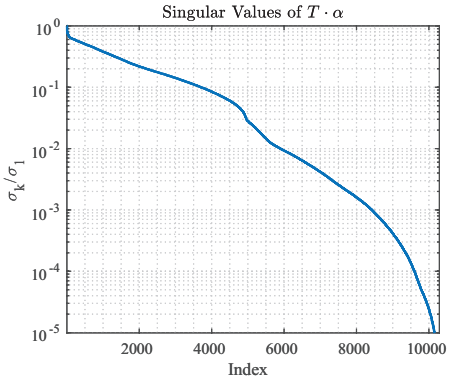

(a) (b) (c)

Figure 4. Compression ratios for different geometries of collections of spheres. (a) Geometries. (b) Parameters and compression ratios. (c) Normalized singular values of the full translation matrix.

from Section 3 to Eq. (21), then the first order solution of the total field will be equal to the incident field, i.e., the Born approximation. On the other hand, the first order solution of the CTMA uses the isolated T-matrices of each object which are complete scattering solutions at the level of the objects. Therefore, the first order solution of the T-matrix system is a stronger first approximation than when the same compression technique is applied to the MoM solution.

5.2. Comparison To The CBFM

In the CBFM [16], the cells of the discretized volume integral equation are first divided into local groups of cells; the geometry is divided into blocks, and blocks are groups of cells. The scattering solution based on the impedance matrix is completed for the cells of each block over multiple plane wave incident fields to yield a set of induced current solutions or volumetric electric fields. The set of induced currents is compressed using a rank-k SVD where the singular vectors of the current distributions are the characteristic basis functions (CBFs). The CBFs are then used to compress each pair-wise interaction sub-matrix between blocks in the impedance matrix as well as the RHS incident fields of the linear system. The resulting compressed system is then solved. A key advantage of the CBFM is that the compressed matrix can be built on the fly. Compression rates in the CBFM can be as good as 1% for homogenous scatterers [27], due to the high redundancy in the MoM matrix in volumetric scattering problems.

The CTMA shares many similarities with the structure of the CBFM. First, the core of the compression lies in a truncated SVD. Second, the right singular vectors, $\mathbf{V}_k$, are used to compress the set of RHS incident fields. Last, the accuracy of the solution and compression ratio is determined by the singular value cutoff threshold. In general, both approaches seek the effective rank of the matrix in order to take advantage of the difference between the true rank and effective rank.

We initially tried to derive basis vectors for the CTMA in a way similar to the CBFM for the scattering from spheres. The idea was to treat each sphere like a block of cells is treated in the CBFM. The scattered field expansion coefficients were computed over multiple plane wave incident fields at the level of individual scatterers. We then took the SVD over the collection of scattered field coefficients and inspected the singular value roll off. We found that essentially no compression was available. The reason for this is that the spherical wave functions form an orthogonal set, and the information contained in each harmonic expansion coefficient is virtually independent. That is, the spherical wave function basis is already highly efficient for isolated spheres, and we expect this to be true for any object for similar reasons. In effect, this process was analogous to trying to compress the basis functions of a Fourier transform.

Unlike the CBFM, the CTMA does not build the compressed linear system on the fly. We must build the entire translation matrix, $\mathbf{T}\boldsymbol{\alpha}$, and apply the SVD to it. Given the block nature of the translation matrix, Eq. (10), it may be possible to apply incremental SVD methods such as [28, 29] to accomplish compression on the fly. In such a scheme, the block translation matrix for one or more scatterers that make up block columns of the full translation matrix would be added to a continually updating truncated SVD. This would allow larger problems to be compressed without storing or operating on the full translation matrix. Exploring this modification is a topic for future work.

5.3. Static Geometries

A variation of the compression scheme can be derived for problems that have the same geometry but different object properties. The T-matrices can be different, but the coordinate frame centers and number of expansion coefficients of each object are the same. A practical example is a parametric sweep over the dielectric constants of a static collection of spheres. Only the full translation matrix is approximated with the SVD, $\boldsymbol{\alpha} \approx \mathbf{U}_k \boldsymbol{\Sigma}_k \mathbf{V}_k^*$, while the block T-matrix, $\mathbf{T}$, is free to change. The solution (18) becomes

$$\mathbf{B} \approx \left(\mathbf{I} + \mathbf{T}\mathbf{U}_k \left(\boldsymbol{\Sigma}_k^{-1} - \mathbf{V}_k^* \mathbf{T} \mathbf{U}_k \right)^{-1} \mathbf{V}_k^* \right) \mathbf{T}\mathbf{A} \tag{22}$$

The singular values and singular vectors of $\boldsymbol{\alpha}$ are computed once and stored then used to form the compressed system for each new set of objects. The same idea can also be applied to the MoM system (21).

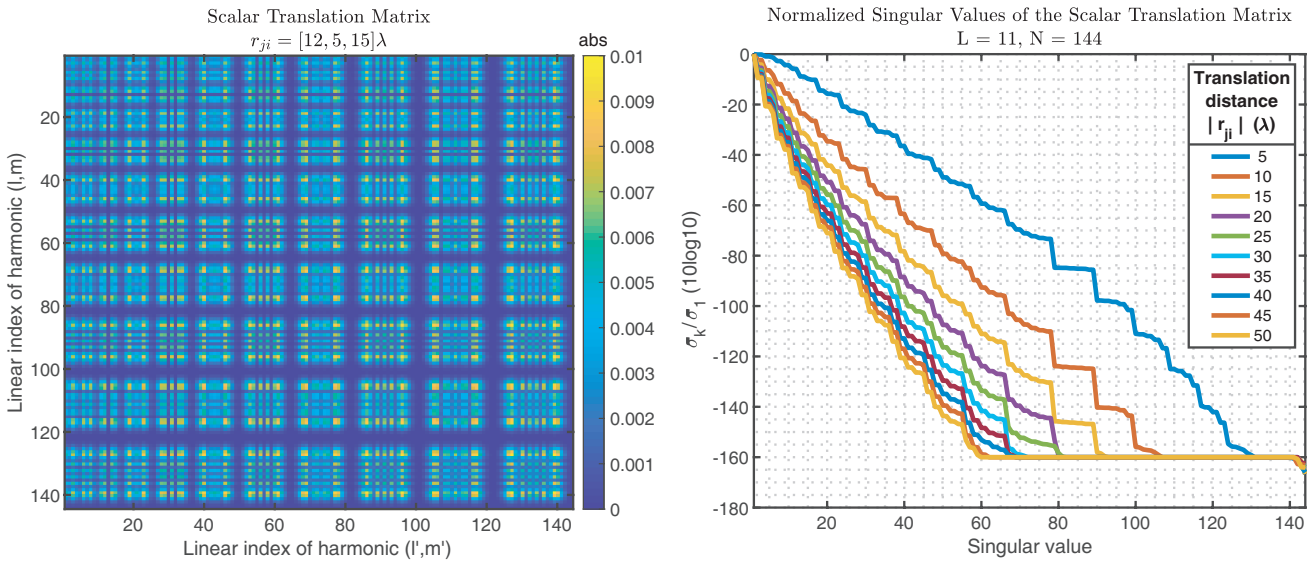

(a) (b)

Figure 5. (a) Scalar translation matrix between two regions with wave function expansion radius of 1.5λ ($L = 11$). (b) normalized SVD singular values of the translation matrix for different magnitudes of translation, r_{ji}. Normalized singular values do not depend on the direction of the translation.

5.4. Compressibility Of Translation Matrices

It is interesting to analyze the compression potential of the translation matrices themselves. This is not what happens in Eq. (15) where the SVD is applied to the entire system of equations which includes multiplication by the object T-matrices. However, this analysis may lead to future insights. The translation matrices contain highly redundant information and can compress to as low as 5% of their original size while retaining accuracy. The compression depends on the size of the object regions and the distance between frame centers. Recall that the number of harmonics needed for translation increases when the size of the objects or expansion regions increases. Figure 5 shows the normalized singular values of $\boldsymbol{\alpha}_{ji}$ for scalar waves for different translation distances for a square translation matrix between two regions that have a radius 1.5λ requiring $L = 11$ and 144 total harmonics. The singular values only depend on the magnitude of the translation, not the direction. This is because the translation matrix is diagonalizable by two rotation matrices that left and right multiply an axial translation matrix. Axial translation only depends on magnitude distance while rotation matrices are unitary, so do not affect the norm of the final matrix. Future T-matrix compression algorithms might take advantage of these observations.

6. CONCLUSIONS

In this work, we derived and tested the Compressed T-matrix Algorithm. The algorithm is based on the SVD and Woodbury identity that were used to compress the T-matrix scattering solution over multiple objects and incident fields. Compression rates as good as 35% were demonstrated over different collections of dielectric spheres with multiple right hand side incident field coefficient vectors. The main drawback of the CTMA is that the SVD must be applied to the entire translation matrix. Future work will investigate incremental SVD algorithms to accomplish the compression on the fly.

ACKNOWLEDGMENT

This research was carried out at the Jet Propulsion Laboratory, California Institute of Technology, under a contract with the National Aeronautics and Space Administration (80NM0018D0004). Copyright 2022. California Institute of Technology. Government sponsorship acknowledged.

REFERENCES

1. Waterman, P. C. and R. Truell, "Multiple scattering of waves," *J. of Math. Phy.*, Vol. 2, No. 4, 512–537, 1961.
2. Chew, W. C., *Waves and Fields in Inhomogeneous Media*, IEEE Press, New York, 1995.
3. Mishchenko, M. I., G. Videen, V. A. Babenko, N. G. Khlebtsov, and T. Wriedt, "T-matrix theory of electromagnetic scattering by particles and its applications: a comprehensive reference database," *J. Quant. Spectrosc. Radiat. Transfer*, Vol. 88, No. 1–3, 357–406, 2004.
4. Koc, S. and W. C. Chew, "Calculation of acoustical scattering from a cluster of scatterers," *J. Acoust. Soc. Am.*, Vol. 103, No. 2, 721–734, 1998.
5. Chew, W. C., L. Gurel, Y.-M. Wang, G. Otto, R. L. Wagner, and Q. H. Liu, "A generalized recursive algorithm for wave-scattering solutions in two dimensions," *IEEE Trans. Microwave Theory and Techniques*, Vol. 40, No. 4, 716–723, 1992.
6. Wang, Y.-M. and W. Chew, "A recursive T-matrix approach for the solution of electromagnetic scattering by many spheres," *IEEE Trans. Ant. Prop.*, Vol. 41, No. 12, 1633–1639, 1993.
7. Chew, W. C., C. Lu, and Y. Wang, "Efficient computation of three-dimensional scattering of vector electromagnetic waves," *JOSA A*, Vol. 11, No. 4, 1528–1537, 1994.
8. Chew, W. and C. Lu, "The recursive aggregate interaction matrix algorithm for multiple scatterers," *IEEE Trans. on Ant. and Prop.*, Vol. 43, No. 12, 1483–1486, 1995.
9. Gumerov, N. A. and R. Duraiswami, "Computation of scattering from N spheres using multipole reexpansion," *J. Acoust. Soc. Am.*, Vol. 112, No. 6, 2688–2701, 2002.

10. Mackowski, D. W. and M. I. Mishchenko, "A multiple sphere T-matrix fortran code for use on parallel computer clusters," *J. Quant. Spec. and Rad. Trans.*, Vol. 112, No. 13, 2182–2192, 2011.
11. Egel, A., L. Pattelli, G. Mazzamuto, D. S. Wiersma, and U. Lemmer, "Celes: CUDA-accelerated simulation of electromagnetic scattering by large ensembles of spheres," *J. Quant. Spec. and Rad. Trans.*, Vol. 199, 103–110, 2017.
12. Siqueira, P. R. and K. Sarabandi, "T-matrix determination of effective permittivity for three-dimensional dense random media," *IEEE Trans. Ant. Prop.*, Vol. 48, No. 2, 317–327, 2000.
13. Maaskant, R., R. Mittra, and A. Tijhuis, "Fast analysis of large antenna arrays using the characteristic basis function method and the adaptive cross approximation algorithm," *IEEE Trans. Ant. Prop.*, Vol. 56, No. 11, 3440–3451, 2008.
14. Um, J. and G. M. McFarquhar, "Optimal numerical methods for determining the orientation averages of single-scattering properties of atmospheric ice crystals," *J. Quant. Spec. and Rad. Trans.*, Vol. 127, 207–223, 2013.
15. Liao, D. and T. Dogaru, "Full-wave scattering and imaging characterization of realistic trees for FOPEN sensing," *IEEE GRSL*, Vol. 13, No. 7, 957–961, 2016.
16. Mittra, R. and K. Du, "Characteristic basis function method for iteration-free solution of large method of moments problems," *Progress In Electromagnetics Research B*, Vol. 6, 307–336, 2008.
17. Zhao, K., M. N. Vouvakis, and J.-F. Lee, "The adaptive cross approximation algorithm for accelerated method of moments computations of EMC problems," *IEEE Trans. on Elec. Comp.*, Vol. 47, No. 4, 763–773, 2005.
18. Mackowski, D. W., "Analysis of radiative scattering for multiple sphere configurations," *Proc. Roy. Soc., Ser. A, Math. and Phys. Sci.*, Vol. 433, No. 1889, 599–614, 1991.
19. Chew, W. C., "Recurrence relations for three-dimensional scalar addition theorem," *Journal of Electromagnetic Waves and Applications*, Vol. 6, No. 1–4, 133–142, 1992.
20. Chew, W. C. and Y. Wang, "Efficient ways to compute the vector addition theorem," *Journal of Electromagnetic Waves and Applications*, Vol. 7, No. 5, 651–665, 1993.
21. Yaghjian, A. D., "Sampling criteria for resonant antennas and scatterers," *J. App. Phys.*, Vol. 79, No. 10, 7474–7482, 1996.
22. Woodbury, M. A., *Inverting Modified Matrices*, Statistical Research Group, 1950.
23. Hager, W. W., "Updating the inverse of a matrix," *SIAM Rev.*, Vol. 31, No. 2, 221–239, 1989.
24. Tsang, L., J. Kong, and K. Ding, *Scattering of Electromagnetic Waves, Vol. 1: Theory and Applications*, Wiley Interscience, New York, 2000.
25. Haynes, M. S., *Waveport Scattering Library*, Jet Propulsion Laboratory, California Institute of Technology, 2021, https://doi.org/10.48588/JPL.HE9D-BA55, https://github.com/nasa-jpl/Waveport.
26. Peterson, A. F., S. L. Ray, R. Mittra, I. of Electrical, and E. Engineers, *Computational Methods for Electromagnetics*, Vol. 2, IEEE Press, New York, 1998.
27. Fenni, I., Z. S. Haddad, H. Roussel, K.-S. Kuo, and R. Mittra, "A computationally efficient 3-D full-wave model for coherent EM scattering from complex-geometry hydrometeors based on MoM/CBFM-enhanced algorithm," *IEEE TGRS*, Vol. 56, No. 5, 2674–2688, 2017.
28. Brand, M., "Incremental singular value decomposition of uncertain data with missing values," *Euro. Conf. Comp. Vis.*, 707–720, Springer, 2002.
29. Baker, C. G., K. A. Gallivan, and P. Van Dooren, "Low-rank incremental methods for computing dominant singular subspaces," *Lin. Alg. App.*, Vol. 436, No. 8, 2866–2888, 2012.